Peptide-specific antibodies localize the major lipid binding sites of talin dimers to oppositely arranged N-terminal 47 kDa subdomains

Gerhard Isenberg[a,*], Wolfgang H. Goldmann[b]

[a] *Biophysics Department E-22, Technical University of Munich, James-Franck Strasse, D-85747 Garching, Germany*
[b] *Department of Medicine, Massachusetts General Hospital, Harvard Medical School, Charlestown, MA 02129, USA*

Received 24 February 1998

Abstract Using ultrastructural analysis and labeling with polyclonal antibodies that recognize peptide sequences specific for phospholipid binding, we mapped the functional domain structure of intact platelet talin and its proteolytic fragments. The talin dimer, which is crucial for actin and lipid binding, is built of a backbone containing the 200 kDa rod portions, at both ends of which a 47 kDa globular domain is attached. Peptide-specific polyclonal antibodies were raised against three potential lipid binding sequences residing within the N-terminal 47 kDa domain (i.e. S19, amino acids 21–39; H18, amino acids 287–304; and H17, amino acids 385–406). Antibodies H17 and H18 localize these lipid binding sequences within the N-terminal 47 kDa globular talin subdomains opposed at the outer 200 kDa rod domains within talin dimers. Hence, we conclude that in its dimeric form, which is used in actin and lipid binding, talin is a dumbbell-shaped molecule built of two antiparallel subunits.

Key words: Electron microscopy; Lipid binding site; Peptide-specific antibody; Talin

1. Introduction

Talin is a highly conserved, widespread protein, first identified as a major protein in focal cell adhesions [1] and subsequently found also in the leading edge of moving cells [2]. Its striking co-localization with nascent actin filament networks and bundles which are formed during cell protrusion prompted us to investigate the binding of talin to actin [3]. Using stopped-flow kinetics, we showed that talin binds G-actin with a K_d of 0.3×10^{-6} M and at a rate of 7×10^{6} M^{-1} s^{-1}, and dissociates 2–3 molecules per second. Independently, Muguruma et al. [4] used gel filtration to demonstrate the binding of talin to actin. When analyzing actin polymerization in the presence of talin at pH 8.0 and various ionic conditions, we found that talin promotes actin filament nucleation by a factor of around 2.5 regardless of whether actin-ATP [5,6] or actin-ADP [7] is used. Moreover, it is known that talin at pH 6.4 and low ionic strength acts as a crosslinking and bundling protein, linking individual actin filaments into three-dimensional networks [8–10]. Based on its primary sequence, three potential actin binding regions have been mapped along the talin sequence [11,12], the C-terminal and the N-terminal regions being the most conserved [11]. Which of the three sites contributes to the various functions of actin binding has not yet been determined. However, although we have been unable to demonstrate any functional actin binding activity in the N-terminal 47 kDa head portion of the talin molecule, we do know that the actin nucleating and actin crosslinking activities remain intact in the 200 kDa C-terminal tail fragment [10,13].

The partial extraction of talin from membrane preparations prompted our investigation of its lipid binding capacity. A combination of biochemical and biophysical techniques enabled us to reliably document a stable interaction of talin with phospholipid membranes. For example, using differential scanning calorimetry (DSC) we were able to discriminate electrostatic adsorption from hydrophobic insertion during the interaction of intact talin with lipid vesicles [14]. The hydrophobic insertion into at least one half of the hydrophobic lipid bilayer was confirmed by the application of photoactivatable lipid analogues (hydrophobic lipid photolabeling), which selectively react with protein domains only when inserted into the hydrophobic part of lipid membranes [6]. Moreover, the binding of talin to lipid surfaces is greatly enhanced in the presence of negatively charged phospholipids. This was demonstrated for DMPC/DMPG lipid mixtures using FTIR with one partner deuterated (DMPC-d54) [14], and for mixed DPPC/DMPG monolayers where talin was observed to segregate into regions rich in negatively charged phospholipids [15]. The molar affinity of talin to lipids (K_d $\sim$0.3 μM) resembles that of moderate protein-protein interactions [16].

Given the apparent sequence homology ($>$40%) with the membrane and actin binding proteins 4.1 and ezrin [17], it has been speculated that the lipid binding domain resides in the smaller 47 kDa calpain II cleavage product [18]. Indeed, we have confirmed by a combination of functional and analytical assays that the 47 kDa head portion harbors an exposed lipid binding domain [13]. Though the 200 kDa talin rod domain exhibits a repetitive hydrophobic core pattern consisting of repeated motifs of amphiphilic α-helices [19], it seems unlikely that further lipid binding domains are exposed on the rod portion, since out of a mixture of 47 kDa and 200 kDa fragments only the 47 kDa domain bound to lipid vesicles [13].

There is evidence that purified talin exists in an equilibrium between monomers and dimers [20]. The dimer configuration, which is functional during actin interaction, is represented ultrastructurally by a dumbbell-shaped homodimer, 51 nm in length and with an antiparallel arrangement of its two monomers [21]. Whereas quantitative dimerization of talin [21] has been confirmed by employing the zero-length crosslinker EDC [22], there is still controversy over the antiparallel [21] or parallel [22] arrangement of subunits within the dimer. By determining that the two functionally different domains, the 47 kDa membrane binding domain and the actin binding

*Corresponding author. Fax: (49) (89) 28912469.

Abbreviations: DMPC, 1,2-dimyristoyl phosphatidylcholine; DMPG, 1,2-dimyristoyl phosphatidylglycerol; DPPC, 1,2-dipalmitoyl-*sn*-glycero-3-phosphatidylcholine

This work is dedicated to Prof. Dr. Karl-Ernst Wohlfarth-Bottermann who died on 29 September 1997.

PII S0014-5793(98)00336-6

rod portion, can be ultrastructurally attributed to distinct regions of the talin homodimer, we provide strong evidence in favor of an antiparallel orientation of talin subunits.

Using data gathered by electron microscopic analysis of the thrombin cleavage products of talin and the application of monospecific affinity purified polyclonal antibodies raised against synthetic peptides which by computer-assisted structure predictions have been designated to carry the three most likely lipid binding motifs within the 47 kDa talin subfragment [23], we here present the first structural evidence for the functional domain arrangement within the talin homodimer. Based on this structural domain organization of the functional talin molecule, we present a model of the orientation of talin within the lipid plasma membrane.

Taken together, our data are in line with the concept that talin is a key molecule for anchoring actin filaments to the lipid membrane at cell/matrix junctions and for nucleating actin assembly at the membrane interface of leading edges [24]. For the gradual evolution of this concept, see [25–28].

2. Materials and methods

2.1. Proteins

Talin was purified from outdated human platelets to homogeneity as judged by SDS-PAGE (cf. Fig. 1) [5], and the protein concentrations were determined as described by Bradford [29]. Purified talin in buffer B (50 mM Tris-HCl pH 8; 0.3 mM EDTA, 0.1 mM DTT) was digested by thrombin (0.5 U/mg protein) at room temperature. After 40 min of digestion, benzamidine (final concentration 10 mM) was added, and the cleavage products were separated on an FPLC anion exchange column (Mono Q, Pharmacia Fine Chemicals) with a linear gradient of 0–800 mM NaCl in buffer B. The 47 kDa fragment is recovered from the flow-through, whereas the 200 kDa domain elutes at 500 mM NaCl.

2.2. Synthetic peptides

The following three peptides, with the highest lipid binding probability according to computer-assisted structure predictions [23], were synthesized on the basis of the mouse talin sequence: residues 21–39: PSTMVYDACRMIRERIPEA (S19; MW 2236.66); residues 287–304: GQMSEIEAKVRYVKLARS (H18; MW 2064.46); residues 385–406: GEQIAQLIAGYIDIILKKKKSK (H17; MW 2457.02).

All peptides were verified by mass spectroscopy; the purity was $>80\%$. For immunization, 2 mg of peptide was coupled to 2 mg of keyhole limpet hemocyanin (KLH) as carrier. The conjugate was separated on a Sephadex G-25 column and stored in PBS at 4 mg/ml.

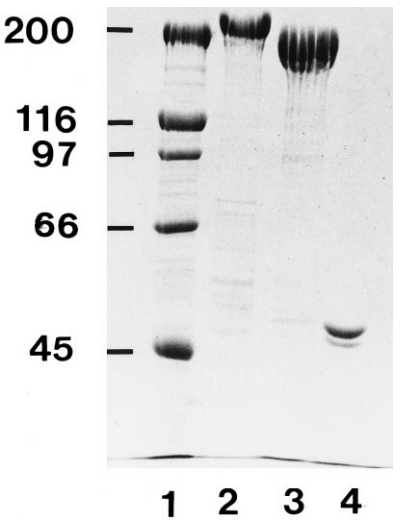

Fig. 1. SDS-PAGE of human platelet talin and its proteolytic fragments. 3 μg of protein was loaded per lane. Intact talin (lane 2); C-terminal 200 kDa rod fragment (lane 3); and 47 kDa N-terminal head fragment (lane 4). For calibration, MW standards have been included as indicated (lane 1). Corresponding samples were viewed by transmission electron microscopy after glycerol spraying/low-angle rotary metal shadowing (cf. Fig. 2).

2.3. Peptide-specific antibodies

New Zealand white rabbits (2.0–2.5 kg) were immunized with 300 μg immunogen each in 300 μl PBS and 1 ml adjuvant sequentially into lymph nodes, intramuscular and subcutaneously. Monospecific IgGs were isolated from 10 ml serum on a CNBr-Sepharose affinity column to which 2–3 mg of the specific peptide had been coupled.

2.4. Electron microscopy

For glycerol spraying/low-angle rotary metal shadowing, we processed protein samples as described in detail previously [21]. Briefly, 0.1–0.3 mg/ml talin in 30% glycerol was sprayed onto freshly cleaved mica, dried under vacuum at room temperature for 1 h and rotary metal-shadowed at an elevation angle of 3–5° with platinum/carbon. For antibody labeling, an aliquot of talin was incubated for 90 min at room temperature with various amounts of the affinity purified IgG up to a 1:1 molar ratio. Specimens were viewed in a Hitachi H-8000 transmission electron microscopy (TEM) operated at 100 kV. Electron micrographs were recorded on Kodak SO-163 electron image film at a nominal magnification of $\times 50\,000$.

3. Results

3.1. Morphology of intact talin and its proteolytic fragments

Thrombin cleavage of talin yields two fragments of 200 kDa and 47 kDa, respectively (Fig. 1). These subunits represent the N-terminal membrane binding head portion (47 kDa) and the actin interacting C-terminal rod domain [13]. Fig. 2 reveals the corresponding electron micrographs of the total native talin molecule and the purified fragments. Consistent with previous documentation, here native talin appears as a dumbbell-shaped elongated molecule with a condensed globular structure at opposite ends of the homodimer (Fig. 2a). When viewing the purified 200 kDa rod domain (Fig. 2b) these protein portions appear as elongated structures with dimensions comparable to the native protein (51 nm) but with a statistically significant loss of the two globular end domains. Likewise, when viewing the purified 47 kDa subdomain (Fig. 1, lane 4), the globular structures, which in density and size compare well with the oppositely arranged condensed regions in the intact molecule, are the only visible structures in these preparations (Fig. 2c).

3.2. Labeling intact talin with peptide-specific antibodies

All three sequence stretches which have been predicted to contain potential lipid binding sites [23] reside in the 47 kDa head portion of the talin molecule. In a parallel study, it has been confirmed (by calorimetry, monolayer studies and CD spectroscopy) that indeed the synthetic talin peptides interact with lipid membranes, with a strong preference for peptide H17, residues 385–406 (GEQIAQLIAGYIDIILKKKKSK), as has been assessed by computer-based structure predictions, when taking into account hydrophobic moments, surface-seeking structure formation and α-helix formation (data not shown).

Labeling of native talin molecules with monospecific IgGs which were raised against synthetic peptides and purified on peptide affinity columns is shown in Fig. 3. The unlabeled talin molecule is displayed in Fig. 3a and the antibody alone is shown in Fig. 3b. Incubation of native talin molecules with

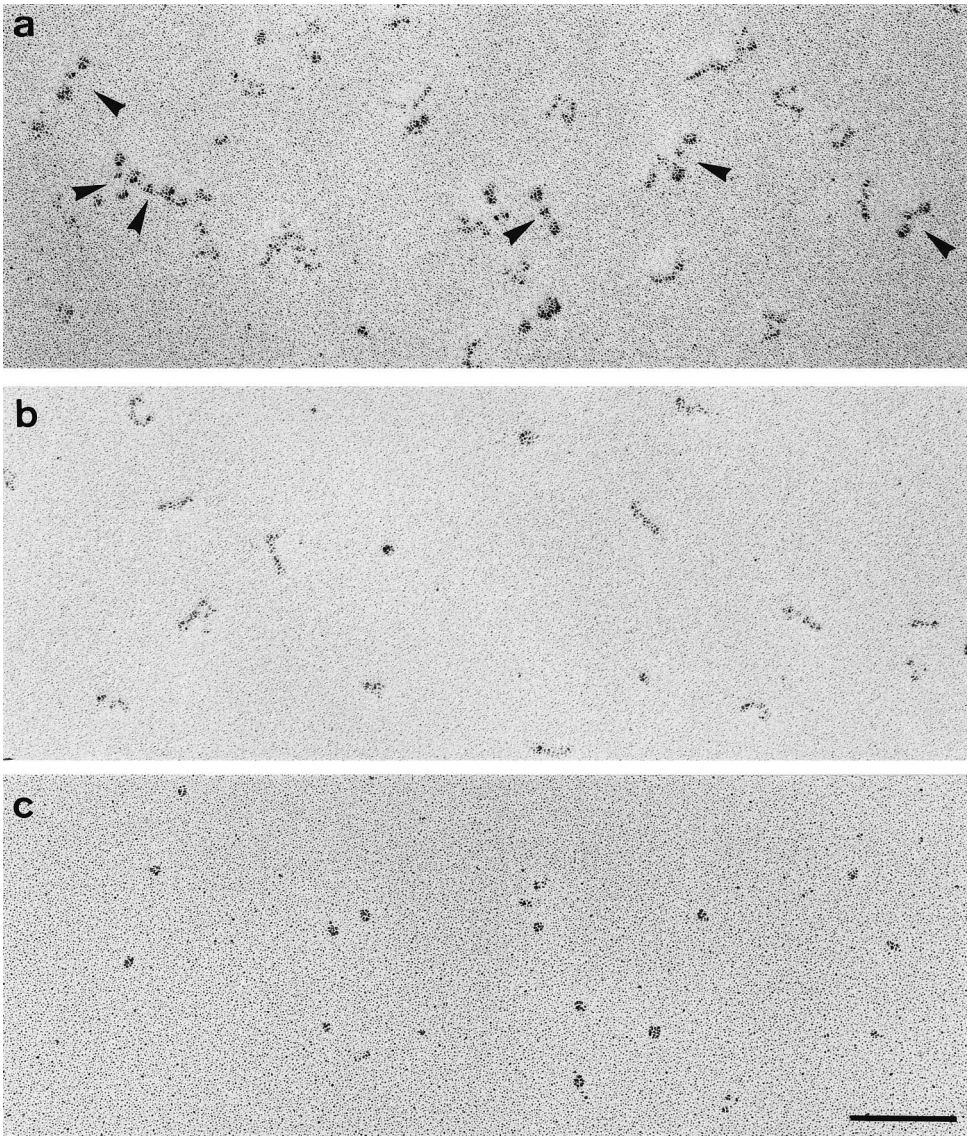

Fig. 2. Ultrastructure of intact talin and its proteolytic fragments as viewed after glycerol spraying, low-angle rotary metal shadowing. a: Intact talin. b: The 200 kDa C-terminal rod fragment. c: The 47 kDa globular N-terminal head fragment. Scale bar, 100 nm (a–c).

antibodies directed against lipid binding sequences within the 47 kDa talin head domain results in labeling as shown in Fig. 3c–f. As documented, we observed exclusive labeling of the globular, oppositely arranged protein domains. When we used a 1:1 molar ratio of antibody to talin, we observed a high background of unbound antibody, indicating a relatively low binding affinity of the antibody for talin. Binding is most commonly observed on either end of the talin homodimer. However, labeling occurred convincingly on both opposite ends simultaneously (Fig. 3e,f). Alternatively, talin molecules were crosslinked by antibodies via their globular end domains. Peptide-specific antibodies raised against H17 and H18 both resulted in a similar labeling, whereas labeling with antibodies directed against peptide S19, carrying the very N-terminal amino acid sequence 21–39, was unsuccessful.

4. Discussion

By combining ultrastructural analysis of intact talin and the 47 kDa as well as the 200 kDa proteolytic fragments of talin and peptide-specific antibody labeling, we were able to map the domain structure of individual talin molecules. Talin is bifunctional in that it can bind to actin via its 200 kDa C-terminal rod portion and simultaneously can anchor to the plasma membrane by its 47 kDa N-terminal head domain by specifically interacting with phospholipids [5,6,13,24, 26,28,30]. So far, it has remained elusive where on the talin molecule these two functional domains reside. It was also of interest to determine how talin might be oriented with respect to the lipid interface and which domain of the talin molecule might be responsible for inserting into the lipid bilayer. As judged by SDS-PAGE, talin is quantitatively cleaved by thrombin into its N-terminal 47 kDa membrane binding domain and its C-terminal 200 kDa rod portion harboring primarily actin binding sites [11–13] but also the integrin [31] and vinculin [32] binding sites.

In agreement with our previously published experimental data [21], we regard the dimer to be the functional configu-

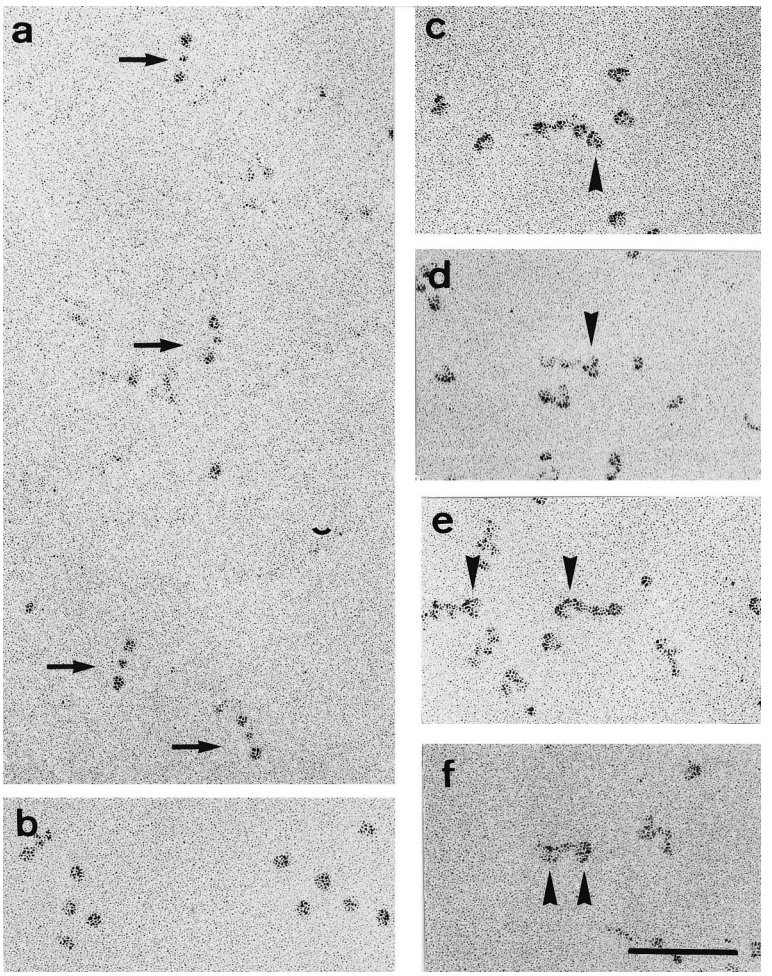

Fig. 3. Labeling of lipid binding sequences within the 47 kDa N-terminal globular head domain by polyclonal peptide-specific antibodies. a: Intact talin molecules. b: Affinity-purified IgG (H18) used for labeling experiments in c–f. Note the difference in size as compared to the 47 kDa globular talin head domain under identical magnification (c–f). Localization of lipid binding epitopes to the 47 kDa globular end of talin dimers, or to both oppositely arranged globular 47 kDa domains simultaneously (f), indicating an antiparallel arrangement of talin within its dimer configuration. Scale bar, 100 nm (a–f).

ration for actin binding. Dimer formation occurs within the 200 kDa C-terminal tail fragments but not within the 47 kDa N-terminal domains [22]. Even GST fusion proteins containing the highly conserved C-terminal actin binding module I/LWEQ migrate exclusively as dimers on gel filtration columns under physiological ionic conditions [33]. We have experimental evidence [10] that the 200 kDa C-terminal domains *alone* are sufficient to crosslink actin filaments into a three-dimensional network. Since the most effective actin binding sites are located at the C-terminal end of the talin rod domain [12,33], it is inconceivable how an actin filament could effectively crosslink into a gel, if talin were a parallel dimer.

Convincing evidence that talin forms antiparallel dimers is found in labeling the 47 kDa membrane binding domain with polyclonal antibodies that have been raised against synthetic peptides representing lipid binding sequences within the 47 kDa N-terminal membrane binding domain. In no case did these antibodies bind to the rod domain. Instead, the antibodies bound to the globular end domains of the dumbbell-shaped talin molecules. Moreover, in no case did we observe two antibodies binding to one and the same globular end domain of the dumbbell-shaped talin molecule. On the other hand, several instances occurred where both globular end domains of the dumbbell-shaped talin molecule were decorated with an antibody. Hence, our data do not support the view of Winkler et al. [22] that talin dimers, according to their energy-filtered electron micrographs, may be arranged in a parallel configuration.

Following our model (Fig. 4), one would further anticipate that talin is anchored in lipid membranes at two sites via its two globular 47 kDa end domains. The rod domain facing the cytoplasm would then allow interaction with actin filaments either by nucleating assembly [5,30] or by crosslinking actin filaments [9,10]. Whether the two actin binding domains within the rod are responsible for the two different functions remains elusive. Since talin has no capping activity, the physical ends of actin filaments would be accessible for the addition of actin monomers. Moreover, in cells the free ends of actin filaments impinge on the membrane with certain average angles. The angle under which protrusion by polymerization would be maximal has been calculated to be $Q = 48°$ [34], which is close to the angle found in situ. We have observed that talin clearly exhibits a flexible hinge region in the middle of the antiparallel, dimeric molecule, thereby allowing for

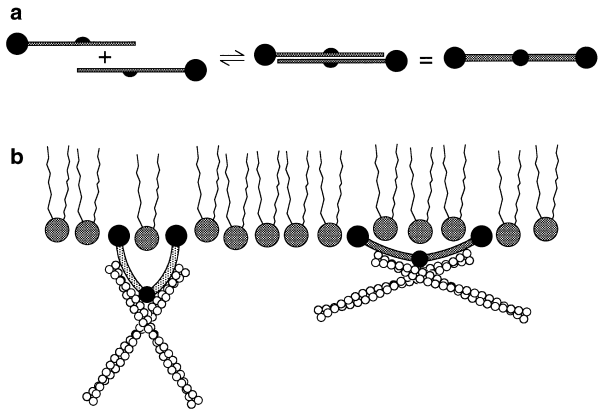

Fig. 4. A model of the talin molecule, representing the structural arrangement of its bifunctional subdomains and its possible orientation at lipid interfaces. This model takes into account the monomer-dimer equilibrium as analyzed by analytical ultracentrifugation as well as the antiparallel arrangement of talin molecules in its dimer configuration (a). The structural backbone of talin dimers consists of the 200 kDa C-terminal rod domain at both ends of which the globular N-terminal head fragment is attached. Since the globular N-terminal fragments harbor the lipid binding sites, talin might anchor to lipid membranes by these globular head portions and simultaneously nucleate actin assembly or crosslink actin filaments via its cytoplasmic oriented C-terminal ends (b). Various kink positions of the highly flexible talin homodimer as a result of different diffusion rates of its globular domains within the plane of the membrane might give rise to different types of actin networks beneath the lipid interface.

various kink positions. Assuming that the lipid binding domains, i.e. the 47 kDa N-terminal end domains are freely diffusible within the plane of the membrane, one would according to this hypothetical model predict that the crosslinking angle of the adjacent actin filament lattice correlates with the diffusion coefficient of the talin lipid binding domains, i.e. when diffusion is restricted due to the assembly of associated proteins, e.g. vinculin and integrins as in focal contacts, the actin filament lattice will be dense resulting ideally in strongly oriented filament cables; when the diffusion rate is enhanced, as in advancing lamellipodium membranes [35], this would result in loose network formation (cf. the hypothetical model in Fig. 4).

Several in vivo observations already support the concept that talin is intimately involved not only in cytoskeleton/membrane anchoring but also in motility regulation. Polyclonal antibodies to talin were found to inhibit cell migration and adhesion on fibronectin when microinjected into fibroblasts [36]. HeLa cells, when down-regulated in talin expression by antisense RNA, also exhibited a reduced rate in cell spreading [37]. More recently, Niewöhner et al. [38] using a talin 'knock-out' strain in *Dictyostelium discoideum* produced a drastically altered phenotype impaired in adhesion and phagocytosis, which is consistent with the importance of talin for the motility behavior of these cells. Finally, microinjection of an antibody (TA 205) that recognizes the N-terminal epitope AA 139–433 in the talin sequence inhibits motility and disrupts stress fibers when injected into chicken embryo fibroblasts [12]. Interestingly, this large sequence region harbors an actin binding domain [11], but it also covers the lipid binding domain AA 385–406, which we have structurally mapped as demonstrated in this report using a peptide antibody directed against this functional site.

The next conceivable step would therefore be to determine the effect of the microinjection of antibodies that recognize lipid binding epitopes on cell motility and cytoskeleton architecture, inasmuch as it has not yet been possible to discriminate whether the talin antibody TA 205 interfered with an actin or with a lipid binding epitope.

Acknowledgements: We thank Dr. S. Kaufmann for protein purification and Ms. Judith Feldmann for careful reading of the manuscript. This work was supported by the Deutsche Forschungsgemeinschaft (Is 25/7-2, SFB 266/C-5, and Go 598/3-1) and North Atlantic Treaty Organization.

References

[1] Burridge, K. and Connell, L. (1983) J. Cell Biol. 97, 359–367.
[2] DePasquale, J.A. and Izzard, C.S. (1991) J. Cell Biol. 113, 1351–1359.
[3] Goldmann, W.H. and Isenberg, G. (1991) Biochem. Biophys. Res. Commun. 178, 718–723.
[4] Muguruma, M., Matsumura, S. and Fukazawa, T. (1990) Biochem. Biophys. Res. Commun. 171, 1217–1223.
[5] Kaufmann, S., Piekenbrock, T., Goldmann, W.H., Bärmann, M. and Isenberg, G. (1991) FEBS Lett. 284, 187–191.
[6] Goldmann, W.H., Niggli, V., Kaufmann, S. and Isenberg, G. (1992) Biochemistry 31, 7665–7671.
[7] Isenberg, G., Niggli, V., Pieper, U., Kaufmann, S. and Goldmann, W.H. (1996) FEBS Lett. 397, 316–320.
[8] Muguruma, M., Matsumura, S. and Fukazawa, T. (1992) J. Biol. Chem. 267, 5621–5624.
[9] Zhang, J., Robson, R.M., Schmidt, J.M. and Stromer, M.H. (1996) Biochem. Biophys. Res. Commun. 218, 530–537.
[10] Goldmann, W.H., Guttenberg, Z., Kaufmann, S., Ezzell, R.M. and Isenberg, G. (1997) Eur. J. Biochem. 250, 447–450.
[11] Hemmings, L., Rees, D.J.G., Ohanian, V., Bolton, S.J., Gilmore, A.P., Patel, B., Priddle, H., Trevithick, J.E., Hynes, R.O. and Critchley, D.R. (1996) J. Cell Sci. 109, 2715–2726.
[12] Bolton, S.J., Barry, S.T., Mosley, H., Patel, B., Jockusch, B.M., Wilkinson, J.M. and Critchley, D.R. (1997) Cell Motil. Cytoskel. 36, 363–376.
[13] Niggli, V., Kaufmann, S., Goldmann, W.H., Weber, T. and Isenberg, G. (1994) Eur. J. Biochem. 224, 951–957.
[14] Heise, H., Bayerl, T., Isenberg, G. and Sackmann, E. (1991) Biochim. Biophys. Acta 1061, 121–131.
[15] Dietrich, C., Goldmann, W.H., Sackmann, E. and Isenberg, G. (1993) FEBS Lett. 324, 37–40.
[16] Goldmann, W.H., Senger, R., Kaufmann, S. and Isenberg, G. (1995) FEBS Lett. 368, 516–518.
[17] Rees, D.G.J., Ades, S.E., Singer, S.J. and Hynes, R.O. (1990) Nature 247, 685–689.
[18] Beckerle, M.C., Burridge, K., Demartino, G.N. and Croall, D.E. (1987) Cell 51, 569–577.
[19] McLachlan, A.D., Stewart, M., Hynes, R.O. and Rees, D.J.G. (1994) J. Mol. Biol. 235, 1278–1290.
[20] Molony, L., McCaslin, D., Abernethy, J., Paschal, B. and Burridge, K. (1987) J. Biol. Chem. 262, 7790–7795.
[21] Goldmann, W.H., Bremer, A., Häner, M., Aebi, U. and Isenberg, G. (1994) J. Struct. Biol. 112, 3–10.
[22] Winkler, J., Lünsdorf, H. and Jockusch, B.M. (1997) Eur. J. Biochem. 243, 430–436.
[23] Tempel, M., Goldmann, W.H., Isenberg, G. and Sackmann, E. (1995) Biophys. J. 69, 228–241.
[24] Isenberg, G. and Goldmann, W.H. (1992) J. Muscle Res. Cell Motil. 13, 587–589.
[25] Isenberg, G. (1991) J. Muscle Res. Cell Motil. 12, 136–144.
[26] Isenberg, G. and Goldmann, W.H. (1995) in: The Cytoskeleton (Hesketh, J. and Pryme, I., Eds.), Vol. I, pp. 169–204, JAI Press, Greenwich.
[27] Isenberg, G. (1996) Semin. Cell Dev. Biol. 7, 707–715.
[28] Isenberg, G. and Niggli, V. (1998) Int. Rev. Cytol. 178, 73–125.
[29] Bradford, M. (1976) Anal. Biochem. 72, 248–254.
[30] Kaufmann, S., Käs, J., Goldmann, W.H., Sackmann, E. and Isenberg, G. (1992) FEBS Lett. 314, 203–205.

[31] Horwitz, A., Duggan, K., Buck, C., Beckerle, M.C. and Burridge, K. (1986) Nature 320, 531–533.
[32] Gilmore, A.P., Wood, C., Ohanian, V., Jackson, P., Patel, B., Rees, D.J.G., Hynes, R.O. and Critchley, D.R. (1993) J. Cell Biol. 122, 337–347.
[33] McCann, R.O. and Craig, S.W. (1997) Proc. Natl. Acad. Sci. USA 94, 5679–5684.
[34] Mogilner, A. and Oster, G. (1996) Eur. Biophys. J. 25, 47–53.
[35] Sheets, E.D., Simson, R. and Jacobson, K. (1995) Curr. Opin. Cell Biol. 7, 707–714.
[36] Nuckolls, G.H., Romer, L.H. and Burridge, K. (1992) J. Cell Sci. 102, 753–762.
[37] Albiges-Rizo, C., Frachet, P. and Block, M.R. (1995) J. Cell Sci. 108, 3317–3329.
[38] Niewöhner, J., Weber, I., Maniak, M., Müller-Taubenberger, A. and Gerisch, G. (1997) J. Cell Biol. 138, 349–361.